Complex Paleozoic magmatic and metamorphic evolution in the Argentera Massif (Western Alps) resolved with U-Pb dating

Autor(en): **Rubatto, Daniela / Schaltegger, Urs / Lombardo, Bruno**

Objekttyp: **Article**

Zeitschrift: **Schweizerische mineralogische und petrographische Mitteilungen = Bulletin suisse de minéralogie et pétrographie**

Band (Jahr): **81 (2001)**

Heft 2

PDF erstellt am: **21.07.2024**

Persistenter Link: https://doi.org/10.5169/seals-61689

SCHWEIZ. MINERAL. PETROGR. MITT. 81, 213–228, 2001

Complex Paleozoic magmatic and metamorphic evolution in the Argentera Massif (Western Alps) resolved with U–Pb dating

by *Daniela Rubatto*[1], *Urs Schaltegger*[2], *Bruno Lombardo*[3], *Fabrizio Colombo*[4] and *Roberto Compagnoni*[4]

Abstract

The timing of pre-Alpine magmatism and metamorphism in the Gesso-Stura Terrain (NE Argentera massif, External Crystalline Massifs) has been investigated by U–Pb dating. Conventional ID-TIMS analysis of zircons from an eclogite constrained the intrusion of the gabbroic protolith at 462 ± 6 Ma, in agreement with an ion microprobe age of 457 ± 6 Ma on the same sample. Regardless of their pristine magmatic zoning, the zircons from the eclogite suffered lead loss during one or more thermal events. A lower discordia intercept (323 ± 12 Ma) and the youngest zircon rim dated by ion-microprobe (330 ± 5 Ma) constrain the age of the last of these events, i. e. the Variscan amphibolite-facies metamorphism, to the Namurian. Zircon from a metadacite indicates that the acid magma crystallised during Late Ordovician at 443 ± 3 Ma. Ion microprobe dating of zircon from a monzonite affected by Variscan anatexis yielded an intrusion age of 332 ± 3 Ma. Our results help reconstructing the pre-Alpine evolution of the Gesso-Stura terrain of the Argentera basement, which records several magmatic and metamorphic events in the time span between Early Ordovician and Late Carboniferous. The zircon behaviour in the dated rocks bears some implications for U–Pb geochronology.

Keywords: U–Pb geochronology, SHRIMP, Argentera, External Crystalline Massifs, eclogite.

Introduction

Our knowledge of the pre-Mesozoic evolution of the Alpine area is limited by two factors: (1) The widespread Alpine overprint that in many terrains deleted most of the pre-Mesozoic mineralogical or structural record; (2) The superposition during the Late Proterozoic and Paleozoic of several magmatic and metamorphic events, which have made overprinting relationships extremely complicated. Therefore, any detail study of pre-Mesozoic geology in the Alps requires a terrain with limited Alpine overprint and has to rely on techniques that can unravel complex geological histories.

This study deals with pre-Mesozoic geology and geochronology in the Argentera massif, the southernmost of the so called "External Crystalline Massifs", a series of basement units aligned along the N and W margin of the Alps (Aar, Gotthard, Tavetsch, Mont Blanc, Aiguilles Rouges, Grandes Rousses, Belledonne, Pelvoux and Argentera; Fig. 1; VON RAUMER et al., 1999; VON RAUMER and NEUBAUER, 1993). In the Argentera massif, Alpine metamorphism is limited to localised mylonitic zones (BOGDANOFF, 1986), ensuring vast preservation of Variscan structure and mineral assemblages, similarly to some parts of the Massif Central in France or of the Moldanubicum of central Europe. In order to unravel

[1] Research School of Earth Sciences, The Australian National University, Canberra ACT 0200, Australia. <daniela.rubatto@anu.edu.au>
[2] Institut für Isotopengeologie und Mineralische Rohstoffe, ETH-Zentrum, Sonneggstrasse 5, CH-8092 Zürich, Switzerland.
[3] CNR, Centro di Studi sulla Geodinamica delle Catene Collisionali, Via Valperga Caluso 35, I-10125 Torino, Italy.
[4] Dipartimento di Scienze Mineralogiche e Petrologiche, Università degli Studi di Torino, Via Valperga Caluso 35, I-10125 Torino, Italy.

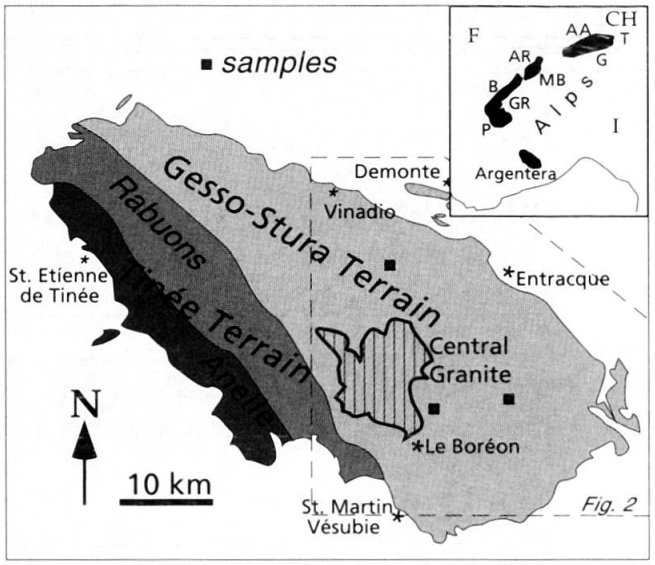

Fig. 1 Geological sketch of the Argentera massif with terrain subdivision. The inset shows the location of the Argentera within the Alps. AA = Aar, AR = Aiguilles Rouges, B = Belledonne, G = Gotthard, GR = Grandes Rousses, MB = Mont Blanc, P = Pelvoux and T = Tavetsch.

the complex sequence of metamorphic and magmatic events in the basement of the Argentera massif, we dated three different metamorphosed igneous rocks by U–Pb zircon geochronology. By using the U–Pb system, which is particularly resistant to thermal overprints, we could avoid resetting caused by Alpine metamorphism and even access the pre-Variscan evolution. Moreover, cathodoluminescence (CL) imaging of the investigated zircon crystals allowed recognising different isotopic domains, recording different geological events. In-situ dating of these zircon domains by SHRIMP ion microprobe, combined with isotope dilution thermal ionisation mass spectrometry (ID-TIMS), led to the reconstruction of a sequence of magmatic and metamorphic events from Early Ordovician to Late Carboniferous. The combination of the different techniques made possible to identify lead loss in apparently pristine zircon crystals, which has important implications for zircon geochronology.

Geological background

The External Crystalline Massifs are portions of polymetamorphic European Variscan crust that were involved in crustal thinning and passive margin formation in the Mesozoic. They were exhumed from below the pile of Alpine sedimentary nappes in the Miocene, during the last stages of Alpine orogeny (VON RAUMER et al., 1999). The Argentera is the southernmost of these massifs (Fig. 1). It crops out as an elliptical body of 60×30 km trending NW–SE. The basement units lay subvertical and run parallel to the main axis of the massif (BOGDANOFF, 1986). The basement mainly consists of migmatites that preserve abundant relics of pre-anatectic rock types. The high temperature (HT) foliation is cross cut by the Central Granite, a large granitic body occurring in the centre of the massif. A second granitic body, which runs sub-parallel to the HT regional foliation, occurs in the NW part of the massif.

Modern geological maps of the Argentera massif (FAURE-MURET, 1955; MALARODA, 1970, 1999) provide good lithological information, but lack a coherent lithostratigraphy for the northern sector of the massif. For this reason, we adopt a new subdivision of the Argentera massif that will be discussed in more detail elsewhere (LOMBARDO et al. in preparation). This subdivision is based on two major terrains named after the valley where they are best exposed: the Gesso-Stura Terrain (GST) and the Tinée Terrain (Fig. 1). The samples investigated are from the Gesso Valley within the GST. The GST roughly corresponds to the Malinvern-Argentera Complex of MALARODA (1970) and comprises the Chastillon-Valmasque and Malinvern Complexes of FAURE-MURET (1955). It extends on the eastern part of the massif and is separated from the Tinée Terrain to the SW by the Ferriere-Mollieres shear zone. In the Gesso Valley, the GST consists mainly of paragneisses and migmatitic orthogneiss, the so-called "anatexite" of MALARODA (1970). Dacitic to rhyodacitic metavolcanic rocks have been recognised throughout the GST (BIERBRAUER, 1995; COLOMBO et al., 1993; GHIGLIONE, 1990; MALARODA, 1991, 1992, 1996, 1999). Intrusive bodies vary from basic (Bousset-Valmasque Complex in the SE; i.e. the Granite of the Valmasque of FAURE-MURET, 1955) to granitic (the Central Granite; FERRARA and MALARODA, 1969) in composition. Small lenses of mafic (metagabbro, granulite and eclogite) and ultramafic rocks are widespread in the whole GST.

Field and petrological evidence shows that the GST records a long geological history (BOGDANOFF, 1986). The oldest rock sequence so far recognised is a pelitic-psammitic sequence with rare carbonatic layers of unknown age. This sequence was intruded by large granitic bodies, which were then completely transformed into migmatites in Variscan times. This basement was later intruded by mafic magmas and covered by dacites, whose relative and absolute age is investigated in this paper. A major metamorphic event at the eclogite/granulite-facies transition (E/G-facies) produced eclogite-facies assemblages in the mafic rocks and garnet-kyanite (high pres-

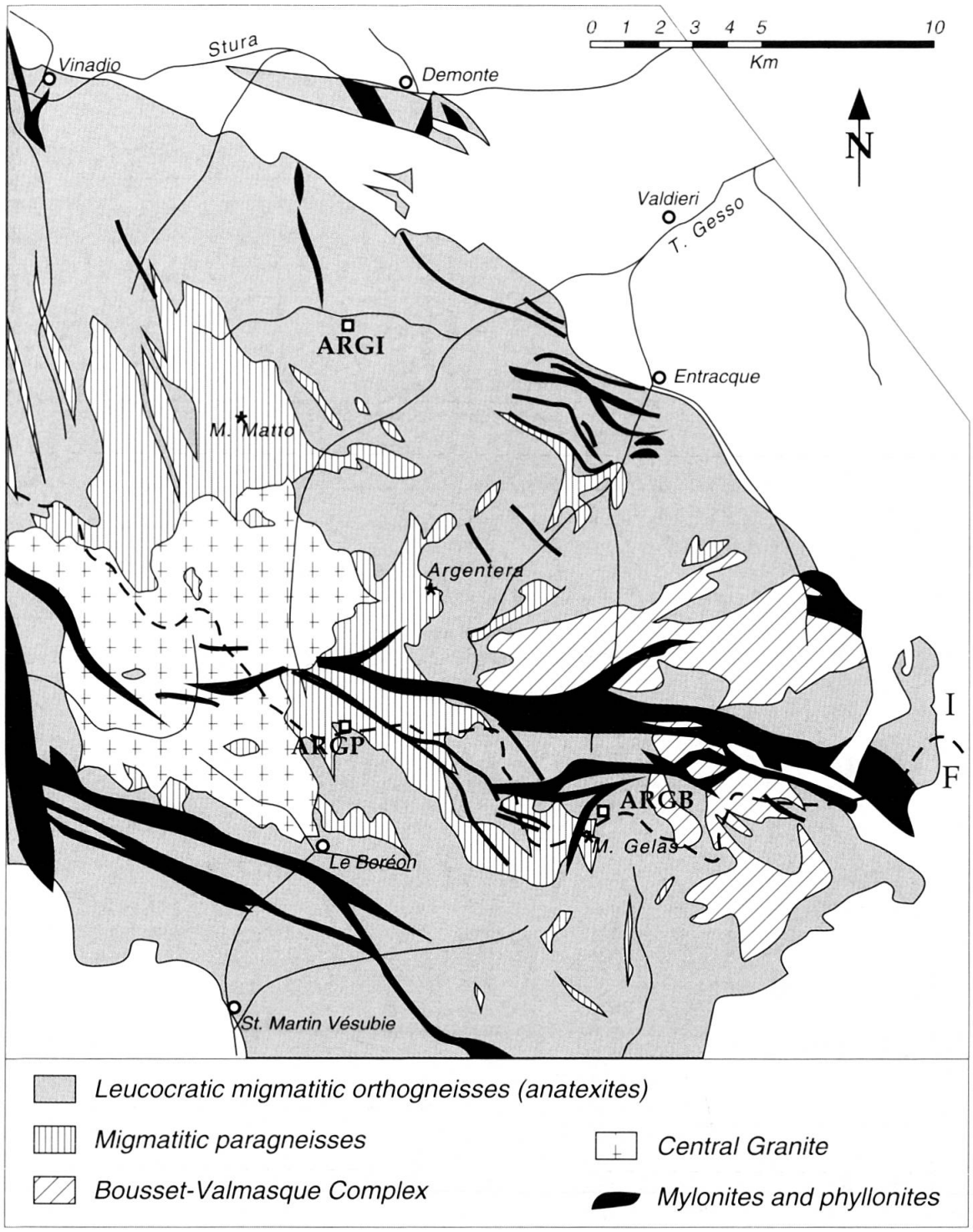

Fig. 2 Geological map of the Gesso-Stura Terrain with sample location.

sure, HP) granulite in the sedimentary, granitic and possibly dacitic rocks. This is especially clear in the banded metabasites of Lago Frisson, where mafic eclogites (plagioclase-free) are interlayered with garnet-omphacite-plagioclase granulites of intermediate composition. Thermobarometry of such assemblages yielded peak equilibration temperatures above 800 °C and pressures around 1.6–1.8 GPa (LOMBARDO et al., 1997). A younger magmatic cycle is represented by the emplacement of monzonitic dykes and bodies, and mafic magmas (the Bousset-Valmasque Complex), both lacking evidence of E/G-facies metamorphism. A major reworking occurred during the Variscan orogeny at low pressure-HT conditions associated to widespread partial melting. Upper Carboniferous sediments (FAURE-MURET, 1955) and the Early Permian intrusion of the Central Granite (FERRARA and MALARODA, 1969) closed the Variscan tectonometamorphic cycle.

Analytical techniques

Zircons for SHRIMP analysis were prepared as mineral separates mounted in epoxy and polished down to expose the grain centres. The selection of zircons for SHRIMP analysis was done on the basis of the CL images. CL investigations were carried out at the CamScan 4 scanning electron microscope at the Institut für Metallforschung und Metallurgie at the ETH in Zürich. Operating conditions were 13 kV and 120 μA. U, Th and Pb analyses were performed with the sensitive high resolution ion microprobes (SHRIMP I and II) at the Research School of Earth Sciences (RSES) in Canberra. Instrumental conditions and data acquisition were generally as described by COMPSTON et al. (1992). The data were collected in sets of seven scans throughout the masses and a reference zircon was analysed each fourth analysis. The measured $^{206}Pb/^{238}U$ ratio was corrected using ref-

Tab. 1 Whole rock chemical analyses of the dated rocks.

	Metadacite	Eclogite	Metamonzonite
SiO_2	66.57	49.55	54.78
TiO_2	0.71	1.73	1.42
Al_2O_3	16.29	17.51	14.08
Fe_2O_3	4.53	9.76	7.07
MnO	0.06	0.16	0.11
MgO	1.39	6.38	5.73
CaO	2.20	10.39	4.93
Na_2O	3.26	2.77	2.37
K_2O	4.01	0.64	6.77
P_2O_5	0.27	0.50	1.07
Tot	99.29	99.39	98.33
LOI	0.87	1.48	0.94
Rb	143	36	303
Sr	201	406	677
Y	49	28	24
Zr	268	49	350
Nb	17	11	19
Ni	16	80	64
Cu	18	58	22
Zn	68	68	77
Th	21	1	38

Tab. 2 SHRIMP U–Th–Pb data. Errors of isotopic ratios and ages are given at 1σ level.

Label	U (ppm)	Th (ppm)	Th/U	$^{204}Pb/^{206}Pb$	$^{206}Pb/^{238}U$	$^{207}Pb/^{235}U$	AGE 207/235	AGE 206/238
ARGI-1.1	128	56	0.44	0.00003	0.0552 ± 0.0010	0.400 ± 0.022	341 ± 16	346 ± 6
ARGI-2.1	297	212	0.71	0.00001	0.0712 ± 0.0010	0.515 ± 0.019	422 ± 13	443 ± 6
ARGI-5.1	181	148	0.82	0.00070	0.0667 ± 0.0010	0.478 ± 0.023	397 ± 16	416 ± 6
ARGI-6.1	259	209	0.80	0.00001	0.0738 ± 0.0011	0.573 ± 0.022	460 ± 14	459 ± 7
ARGI-6.2	152	67	0.44	0.00008	0.0721 ± 0.0010	0.547 ± 0.019	443 ± 13	449 ± 6
ARGI-7.1	126	55	0.43	0.00018	0.0689 ± 0.0010	0.530 ± 0.021	432 ± 14	430 ± 6
ARGI-8.1	217	69	0.32	0.00027	0.0691 ± 0.0010	0.533 ± 0.019	434 ± 13	431 ± 6
ARGI-9.1	143	69	0.48	0.00001	0.0580 ± 0.0010	0.423 ± 0.021	359 ± 15	363 ± 6
ARGI-9.2	312	230	0.74	0.00018	0.0722 ± 0.0010	0.527 ± 0.022	430 ± 15	450 ± 6
ARGI-10.1	635	310	0.49	0.00010	0.0710 ± 0.0009	0.524 ± 0.015	428 ± 10	442 ± 6
ARGI-10.2	331	292	0.88	0.00006	0.0703 ± 0.0010	0.603 ± 0.024	479 ± 15	438 ± 6
ARGI-11.1	621	380	0.61	0.00015	0.0615 ± 0.0008	0.465 ± 0.016	388 ± 11	385 ± 5
ARGI-13.1	212	96	0.45	0.00001	0.0533 ± 0.0008	0.401 ± 0.018	342 ± 13	335 ± 5
ARGI-13.2 rim	234	104	0.44	0.00001	0.0525 ± 0.0009	0.411 ± 0.025	350 ± 18	330 ± 5
ARGI-14.1	196	74	0.38	0.00034	0.0728 ± 0.0011	0.593 ± 0.025	473 ± 16	453 ± 7
ARGI-15.1	353	114	0.32	0.00001	0.0620 ± 0.0009	0.443 ± 0.017	373 ± 12	388 ± 5
ARGI-16.1	189	67	0.36	0.00005	0.0667 ± 0.0010	0.489 ± 0.015	404 ± 10	416 ± 6
ARGI-17.1	298	144	0.48	0.00001	0.0756 ± 0.0008	0.586 ± 0.012	469 ± 8	470 ± 5
ARGI-18.1 rim	18	1	0.08	0.00470	0.0565 ± 0.0029	0.420 ± 0.094	356 ± 69	354 ± 18
ARGI-18.2	180	87	0.48	0.00292	0.0598 ± 0.0015	0.447 ± 0.029	375 ± 20	374 ± 9
ARGI-19.1	830	520	0.63	0.00002	0.0744 ± 0.0008	0.580 ± 0.013	464 ± 8	463 ± 5
ARGI-20.1 rim	633	120	0.19	0.00001	0.0525 ± 0.0013	0.414 ± 0.017	352 ± 12	330 ± 8
ARGI-20.2	439	199	0.45	0.00054	0.0644 ± 0.0018	0.481 ± 0.022	399 ± 15	403 ± 11
ARGI-21.1	148	57	0.39	0.00096	0.0672 ± 0.0016	0.526 ± 0.030	429 ± 20	419 ± 10
ARGI-21.2	149	60	0.40	0.00069	0.0648 ± 0.0020	0.493 ± 0.033	407 ± 23	405 ± 12
ARGI-25.1	475	497	1.05	0.00074	0.0655 ± 0.0013	0.482 ± 0.024	399 ± 17	409 ± 8
ARGI-28.1	281	104	0.37	0.00121	0.0609 ± 0.0016	0.439 ± 0.022	370 ± 16	381 ± 9
ARGI-29.1	125	58	0.46	0.00016	0.0734 ± 0.0009	0.551 ± 0.016	446 ± 11	456 ± 5
ARGI-32.1	236	85	0.36	0.00127	0.0682 ± 0.0016	0.538 ± 0.024	437 ± 16	425 ± 9
ARGI-32.2	99	40	0.40	0.00183	0.0622 ± 0.0020	0.428 ± 0.058	362 ± 42	389 ± 12
ARGI-33.1	243	112	0.46	0.00007	0.0735 ± 0.0008	0.581 ± 0.013	465 ± 8	457 ± 5
ARGI-40.1	210	72	0.34	0.00011	0.0731 ± 0.0008	0.546 ± 0.011	442 ± 7	455 ± 5
ARGI-40.2	143	96	0.67	0.00007	0.0752 ± 0.0009	0.587 ± 0.019	469 ± 12	468 ± 5
ARGI-41.1	102	49	0.48	0.00028	0.0767 ± 0.0011	0.600 ± 0.022	478 ± 14	476 ± 7

erence zircon from Sri Lanka (SL13). The data were corrected for common Pb on the basis of the measured $^{208}Pb/^{206}Pb$ ratio (COMPSTON et al., 1992). ^{204}Pb was also monitored during the analysis and the common Pb correction based on ^{204}Pb gave similar results to the ^{208}Pb based correction. However, because of the young age of some of the zircon and the low amount of ^{204}Pb measured, the ^{208}Pb corrected data yielded a better precision and are thus preferred. The fact that the zircon standard, which has been proved to be free of intrinsic common Pb, and the samples contained a similar amount of ^{204}Pb (1–20 ppb) is indication that the common Pb is mainly surface and machine Pb. Therefore, the common Pb composition was assumed to be Broken Hill common Pb, which approximates the laboratory common Pb at RSES. In any case, the ages obtained are not significantly affected by the type of common Pb correction or common Pb composition because of the low percent of common Pb in each analysis. The mean ages are weighted means at the 95% confidence level, if not otherwise indicated, while the single data points listed in tables and figures are given with 1σ errors.

The zircons used for conventional U–Pb analysis were air-abraded, washed in warm 4N nitric acid, and rinsed several times with distilled water

Tab. 2 (cont.) SHRIMP U–Th–Pb data. Errors of isotopic ratios and ages are given at 1σ level.

Label	U (ppm)	Th (ppm)	Th/U	$^{204}Pb/^{206}Pb$	$^{206}Pb/^{238}U$	$^{207}Pb/^{235}U$	AGE 207/235	AGE 206/238
ARGP-5.1	204	39	0.19	0.00017	0.0693 ± 0.0010	0.506 ± 0.018	416 ± 12	432 ± 6
ARGP-7.1	275	31	0.11	0.00025	0.0708 ± 0.0010	0.538 ± 0.012	437 ± 8	441 ± 6
ARGP-6.1 core	458	132	0.29	0.00012	0.1148 ± 0.0016	0.998 ± 0.019	703 ± 10	701 ± 9
ARGP-8.1	276	31	0.11	0.00001	0.0699 ± 0.0010	0.527 ± 0.012	430 ± 8	436 ± 6
ARGP-11.1	266	38	0.14	0.00018	0.0720 ± 0.0010	0.556 ± 0.013	449 ± 9	448 ± 6
ARGP-14.1	169	49	0.29	0.00001	0.0722 ± 0.0012	0.570 ± 0.021	458 ± 14	450 ± 7
ARGP-16.1	150	43	0.28	0.00084	0.0731 ± 0.0010	0.557 ± 0.016	449 ± 11	455 ± 6
ARGP-15.1	129	28	0.22	0.00027	0.0736 ± 0.0011	0.560 ± 0.017	452 ± 11	458 ± 6
ARGP-17.1	139	32	0.23	0.00014	0.0690 ± 0.0011	0.505 ± 0.019	415 ± 13	430 ± 6
ARGP-19.1	264	16	0.06	0.00000	0.0704 ± 0.0012	0.550 ± 0.014	445 ± 9	438 ± 7
ARGP-19.2 core	249	67	0.27	0.00007	0.0976 ± 0.0018	0.824 ± 0.023	610 ± 13	600 ± 10
ARGP-20.1	244	42	0.17	0.00002	0.0735 ± 0.0015	0.622 ± 0.017	491 ± 10	457 ± 9
ARGP-20.2 core	511	434	0.85	0.00000	0.4493 ± 0.0074	12.602 ± 0.224	2650 ± 17	2392 ± 33
ARGP-22.1	194	46	0.24	0.00004	0.0705 ± 0.0012	0.537 ± 0.016	437 ± 11	439 ± 7
ARGP-23.1	393	108	0.28	0.00001	0.0969 ± 0.0017	0.809 ± 0.017	602 ± 10	596 ± 10
ARGP-23.2	209	60	0.29	0.00004	0.0910 ± 0.0017	0.755 ± 0.023	571 ± 13	562 ± 10
ARGP-24.1	242	38	0.16	0.00017	0.0696 ± 0.0012	0.555 ± 0.012	448 ± 8	434 ± 7
ARGP-25.1	205	19	0.09	0.00001	0.0707 ± 0.0013	0.545 ± 0.014	442 ± 9	441 ± 8
ARGP-25.2 core	331	170	0.51	0.00002	0.2770 ± 0.0046	4.595 ± 0.085	1748 ± 16	1576 ± 23
ARGP-25.3 core	248	85	0.34	0.00001	0.2981 ± 0.0066	5.224 ± 0.209	1857 ± 35	1682 ± 33
ARGP-26.1	147	55	0.38	0.00010	0.0689 ± 0.0009	0.499 ± 0.016	411 ± 11	430 ± 5
ARGP-27.1	95	71	0.75	0.00034	0.0712 ± 0.0009	0.544 ± 0.022	441 ± 14	443 ± 6
ARGP-29.1	193	29	0.15	0.00027	0.0700 ± 0.0009	0.535 ± 0.011	435 ± 8	436 ± 6
ARGP-31.1	201	45	0.22	0.00001	0.0718 ± 0.0008	0.543 ± 0.013	441 ± 8	447 ± 5
ARGP-31.2	180	39	0.21	0.00009	0.0721 ± 0.0008	0.543 ± 0.013	441 ± 9	449 ± 5
ARGP-32.1	206	141	0.68	0.00003	0.0729 ± 0.0008	0.551 ± 0.013	446 ± 9	454 ± 5
ARGP-33.1	404	58	0.14	0.00020	0.0691 ± 0.0008	0.556 ± 0.009	449 ± 6	430 ± 5
ARGP-34.1	260	27	0.10	0.00003	0.0728 ± 0.0008	0.568 ± 0.010	456 ± 6	453 ± 5
ARGB-1.1	876	389	0.44	0.00002	0.0514 ± 0.0005	0.366 ± 0.006	317 ± 4	323 ± 3
ARGB-1.2	810	410	0.51	0.00001	0.0529 ± 0.0006	0.386 ± 0.007	331 ± 5	332 ± 3
ARGB-3.1	1054	474	0.45	0.00012	0.0544 ± 0.0012	0.400 ± 0.013	341 ± 9	341 ± 7
ARGB-4.1	1211	530	0.44	0.00015	0.0500 ± 0.0009	0.362 ± 0.011	313 ± 8	314 ± 6
ARGB-4.2	701	489	0.70	0.00059	0.0558 ± 0.0011	0.433 ± 0.016	366 ± 12	350 ± 7
ARGB-5.1	1096	462	0.42	0.00025	0.0526 ± 0.0010	0.400 ± 0.012	341 ± 9	330 ± 6
ARGB-6.1	555	272	0.49	0.00001	0.0529 ± 0.0006	0.391 ± 0.007	335 ± 5	332 ± 3
ARGB-7.1	748	312	0.42	0.00003	0.0532 ± 0.0006	0.390 ± 0.006	334 ± 4	334 ± 3
ARGB-8.1	988	413	0.42	0.00006	0.0535 ± 0.0006	0.393 ± 0.007	337 ± 5	336 ± 3
ARGB-9.2	708	322	0.45	0.00047	0.0533 ± 0.0010	0.393 ± 0.012	337 ± 9	335 ± 6
ARGB-10.1	1261	609	0.48	0.00001	0.0497 ± 0.0010	0.378 ± 0.013	326 ± 10	313 ± 6
ARGB-12.1	658	319	0.49	0.00001	0.0525 ± 0.0006	0.384 ± 0.008	330 ± 6	330 ± 4

and acetone in an ultrasonic bath. U–Pb analytical procedures closely follow those described in SCHALTEGGER et al. (1999). Total procedural blanks were 2 pg Pb and 0.05 pg U. A mixed ^{205}Pb–^{235}U tracer solution was used for the analysis. Pb and U were loaded together on single Re filament with Si-Gel and phosphoric acid and measured on a Finnigan MAT 262 mass spectrometer using an ion counting system. Discordia intercepts were calculated using Isoplot/Ex (LUDWIG, 2000).

Geochronological data

ECLOGITE ARGI

A large (600×150 m) mafic body crops out in the Val Meris, in the Italian part of the GST (Fig. 2). The body is elongated parallel to the foliation of the host migmatites from which is separated by late shear zones. The rock chemical composition indicates basaltic liquid composition (Tab. 1).

The Val Meris mafic body displays a series of facies from coarse-grained eclogites to rocks where the eclogite-facies paragenesis is completely replaced by an amphibolite-facies assemblage. The eclogite assemblage consists of garnet, omphacite and quartz, and accessory rutile, apatite and ilmenite. Omphacite is partly to completely replaced by a symplectite of plagioclase with either diopside or amphibole (Fig. 3a). From the jadeite content of omphacite (Jd_{23}) (HOLLAND, 1980) and Fe/Mg partitioning between omphacite and garnet (POWELL, 1985) in the better preserved eclogite, minimum pressures of ~1.6 GPa and equilibration temperatures of ~780 °C were estimated (LOMBARDO et al., 1997).

U–Pb data

Eclogite ARGI contains large zircons with diameter of 300 μm, which are colourless to pale yellow. Most of the zircons preserve crystal faces, but only a few grains are euhedral. In CL the zircons show oscillatory zoning, rarely organised in sectors, with zoning bands parallel to the crystal faces (Figs 4a–b). Few of the zircons have a thin rim (5–25 μm large) with no zoning and very high CL emission (Fig. 4b).

The zircon crystals from this sample were analysed for U–Pb with both ion microprobe and ID-TIMS techniques. With the exception of the bright rims, the zircons contain between 87 and 830 ppm uranium, and 40 to 520 ppm thorium (Tabs 2 and 3), which is not unusual for gabbroic zircon (e.g. RUBATTO et al., 1998; RUBATTO and GEBAUER, 2000). Th/U ratios are between 0.3 and 1, as normally observed in magmatic zircons. The few rims analysed by SHRIMP have significantly lower U and Th contents as well as Th/U ratio (Tab. 2 and Fig. 4b), and might either represent metamorphic overgrowths or be the product of recrystallisation.

More than 30 SHRIMP analyses were carried out in this sample. The apparent $^{206}Pb/^{238}U$ ages range from Middle Ordovician (470 Ma) to Early Carboniferous (330 Ma) with a major cluster at around 460 Ma, a second group of ages at around 425 Ma and a third group at ca. 385 Ma (Fig. 5a and Tab. 2). The 13 oldest analyses that form the major data cluster correspond to zircon cores with typical magmatic zoning. These analyses form a single population ($\chi^2 = 2.9$) that defines a $^{206}Pb/^{238}U$ age of 457 ± 6 Ma. The few zircon rims/overgrowths analysed yield Early Carboniferous ages, with two analyses at 330 Ma, the youngest age obtained in this sample.

The nine ID-TIMS analyses (eight single zircons and one multigrain fraction) also yielded ages ranging from Middle Ordovician to Carboniferous (Tab. 3). On the Concordia diagram, the nine analyses define a discordia line with a relatively bad fit (MSWD = 1) and with upper and lower intercept ages of 471 ± 8 Ma and 322 ± 9 Ma, respectively (Fig. 6). Analysis 1A is concordant at 458.8 ± 0.7 Ma, in agreement with the oldest age group obtained by SHRIMP measurements. A more precise evaluation of the upper intercept age is obtained with the 5 most concordant points (see inset A of Fig. 6), which define an age of 462 ± 6 Ma. Analysis 1X1 may be regarded as slightly biased by inherited lead. Exclusion of this point from the calculation leads to an upper intercept age of 460 ± 4 Ma, which is indistinguishable from the former one, and a lower intercept age of 81 ± 350 Ma. The lower intercept age has been constrained at an age of 323 ± 12 Ma by using the 4 most discordant points (see inset B in Fig. 6), with an apparent upper intersection at ~472 Ma. This leads to the conclusion that the magmatic zircons crystallised at 462 ± 6 Ma and suffered some post-crystallisation lead loss. The Variscan overgrowth occurred at 323 ± 12 Ma and obviously was more resistant to lead loss. The linear array in figure 6 therefore defines an apparent upper intercept age that is overestimating the crystallisation age. The ID-TIMS and SHRIMP ages are thus in perfect agreement (457 ± 6 and 462 ± 6 Ma, respectively) and average at 459 ± 4 Ma (2σ).

Most of the ID-TIMS analyses were performed on zircons that preserve crystal faces, and CL investigation of the grains dated by SHRIMP show that the zircons have magmatic oscillatory zoning. Therefore, it is concluded that the Middle Ordovician age of 459 ± 4 Ma (2σ) constrains the

Tab. 3 ID-TIMS U–Pb data. Errors of isotopic ratios and ages are given at 1σ level.

Analysis a)	Weight [mg]	Concentrations U [ppm]	Pb rad. [ppm]	Pb nonrad. [pg]	Th/U b)	Atomic ratios 206/204 c)	206/238 d)	Error 1σ	207/235 d)	Error 1σ	207/206 d)	Error 1σ	Apparent ages 206/238	207/235	207/206
ARGI/1 1g	0.0245	142	9.47	13.3	0.46	1083	0.06429	± 0.00015	0.4883	± 0.0012	0.05508	± 0.00009	401.7	403.7	415.5
ARGI/1A 1g	0.0195	166	12.50	7.9	0.41	1922	0.07377	± 0.00012	0.5713	± 0.0012	0.05616	± 0.00006	458.8	458.8	458.8
ARGI/1B 1g	0.0296	136	7.37	3.4	0.36	4049	0.05405	± 0.00010	0.3980	± 0.0009	0.05340	± 0.00007	339.4	340.2	345.8
ARGI/1C 1g	0.0277	118	7.72	7.3	0.40	1836	0.06429	± 0.00014	0.4881	± 0.0013	0.05506	± 0.00009	401.6	403.6	414.8
ARGI/2 6g	0.0049	205	15.43	6.5	0.54	708	0.07107	± 0.00014	0.5503	± 0.0019	0.05616	± 0.00016	442.6	445.2	458.6
ARGI/3 1g	0.0095	118	8.72	8.8	0.41	598	0.07219	± 0.00023	0.5581	± 0.0025	0.05607	± 0.00022	449.3	450.3	455.0
ARGI/1X3 1g	0.0272	114	6.99	2.2	0.41	5467	0.05982	± 0.00010	0.4495	± 0.0009	0.05450	± 0.00005	375.6	376.9	391.6
ARGI/1X1 1g	0.0143	87	6.64	1.8	0.46	3256	0.07356	± 0.00012	0.5713	± 0.0013	0.05633	± 0.00008	457.5	458.9	465.5
ARGI/1X2 1g	0.0148	460	12.25	1.7	0.51	6505	0.07309	± 0.00012	0.5664	± 0.0011	0.05621	± 0.00005	454.7	455.7	460.5

a) 1g = single grain fraction; 6g = 6 grains fraction
b) Calculated on the basis of radiogenic Pb208/Pb206 ratios, assuming concordancy
c) Corrected for fractionation and spike
d) Corrected for fractionation, spike, blank and common lead (STACEY and KRAMERS, 1975)

intrusion of the magmatic protolith of the eclogite. The abundance of zircon found in this sample suggests that the protolith magmatic rock was a gabbro rather than basalt, because in basalts fast cooling generally prevents zircon crystallisation (RUBATTO et al., 1998). This is in agreement with the cm- to dm-thick banding of the rock, its coarse grained texture (Fig. 3a) and chemical composition (Tab. 1).

The zircon rims represent either recrystallised domains or overgrowths, both commonly observed in metamorphic rocks. Unfortunately, their limited abundance and small size prevented from the precise determination of their age, even using ion microprobe. However, the youngest ages obtained on zircon rims (~330 Ma) still define a likely maximum age for the last metamorphic event that the rock records, i.e. the Variscan amphibolite-facies metamorphism. This age is supported by the lower intercept at 323 ± 12 Ma defined by the ID-TIMS analyses. The age measurements do not furnish any direct information on the age of the eclogitic metamorphism recorded by the rock. It could be speculated that the young shoulder of the 459 Ma peak (at ~440 Ma) or the apparent age clusters detected by ion microprobe at ~425 Ma and ~385 Ma are somehow related to metamorphism. However, the possibility of mixed ages due to partial Pb loss cannot be ruled out and thus the interpretation of these "clusters" remains dubious.

METADACITE ARGP

This rock type is found in the south part of the GST, in the Val Meris and in the ridge between Cima Ghiliè and Testa della Rovina (ROMAIN, 1982, p. 30; GHIGLIONE, 1990; COLOMBO et al., 1993; BIERBRAUER, 1995). The large outcrop found at Cima Ghiliè (Vallone della Rovina) is reported in the 1:50000 geological map of the Argentera massif as "paleo-cataclasites" (MALARODA, 1970). Similar rocks have been described on the French part of the massif as "pseudo porphyric gneisses" (MALARODA, 1991, 1999). The term metadacite is used in this paper because of the porphyritic texture in the undeformed sample (Fig. 3c), the presence of xenoliths and the chemical composition (Tab. 1). The parental magma can be classified as S-type according to its high aluminium saturation index (CHAPPELL and WHITE, 1992).

At Cima Ghiliè, undeformed metadacites progressively pass to deformed rocks with gneissic texture, which have transitional contact to the surrounding migmatites, which are likely to be Varis-

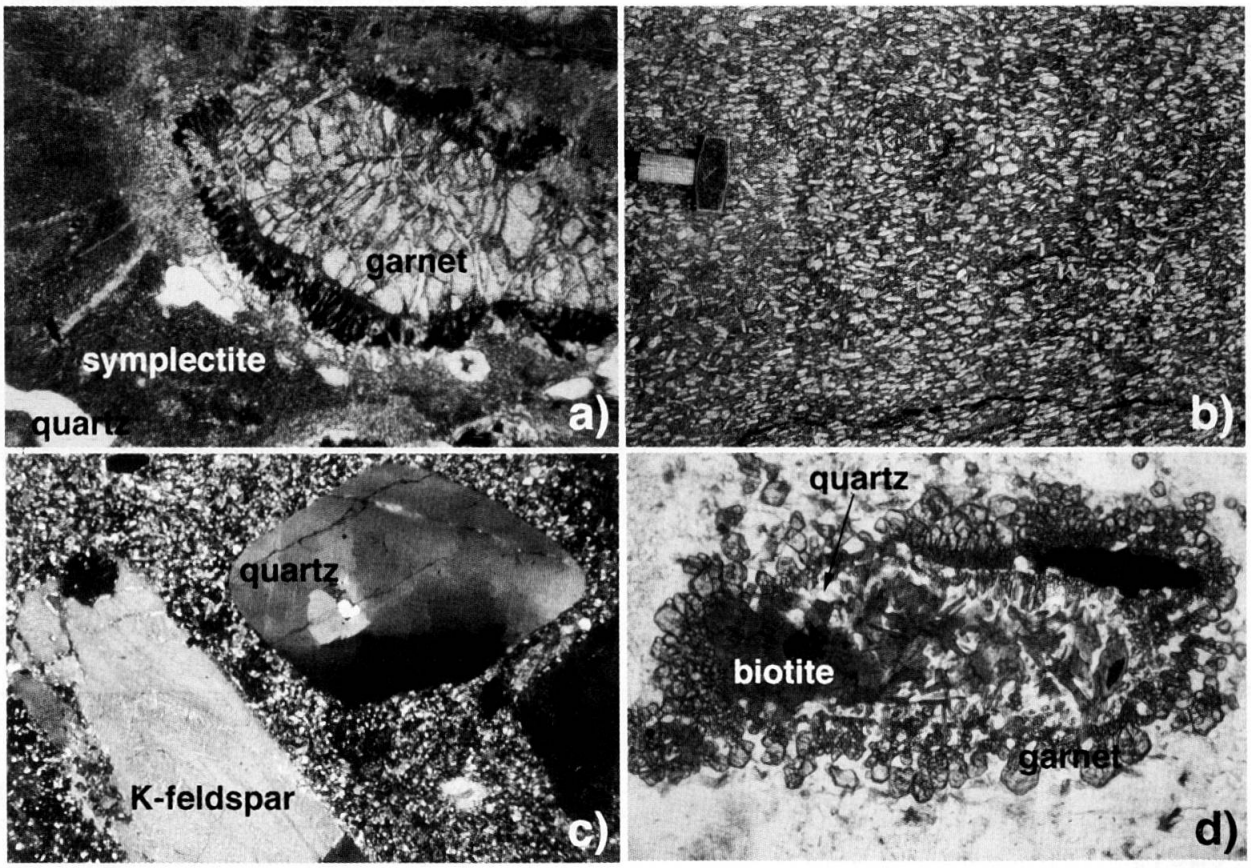

Fig. 3 (a) Photomicrograph of eclogite ARGI with symplectite of plagioclase with either diopside or amphibole on previous omphacite. The garnet is surrounded by a retrograde corona of green hornblende with sericite + epidote on previous plagioclase. Base of picture 5 mm. (b) Metamonzonite ARGB preserving magmatic texture. (c) Photomicrograph of a metadacite preserving volcanic texture. Base of picture 5 mm. (d) Photomicrograph of metadacite ARGP showing coronitic garnet on biotite-quartz aggregate, which is most probably derived from a previous xenocrystal of orthopyroxene. Base of picture 1.25 mm.

can (GHIGLIONE, 1990; BIERBRAUER, 1995). The undeformed metadacite preserves magmatic phenocrysts of quartz, plagioclase, K-feldspar, biotite and altered cordierite (Fig. 3c). The microcrystalline matrix contains quartz, feldspars and aggregates of biotite and quartz, which are most probably derived from previous xenocrystals of orthopyroxene (Fig. 3d). The cordierite phenocrysts are completely substituted by pinite and surrounded by euhedral metamorphic garnets also present as coronas around retrogressed orthopyroxene (Fig. 3d). The garnet corona is not magmatic as garnet also formed in the marginal part of the metadacite body (BIERBRAUER, 1995). Here the undeformed metadacite passes into a foliated blastomylonite ("Streifengneis" of BIERBRAUER, 1995) in which plagioclase, K-feldspar, quartz and garnet are in equilibrium. On structural grounds, BIERBRAUER (1995) showed that the transformation of the dacite into blastomylonite is older than the Variscan anatexis. It is likely that the paragenesis described by BIERBRAUER (1995) and thus the coronitic garnet in the dacite are the product of an HP granulitic event prior to Variscan amphibolite-facies metamorphism. Additionally to the garnet corona on biotite in the matrix, the metadacite contains frequent xenoliths mainly consisting of granulite-facies metapelites, which document granulite-facies metamorphism in the mid-lower crust prior to or even coeval with the event that produced the dacitic melt and distinct from the later HP granulitic event which transformed the dacite into blastomylonite.

U–Pb data

The metadacite contains pink, euhedral zircons that are generally elongated with length-width ratios around 2.5. In CL the zircons show two distinct crystallographic domains (Fig. 4c): composite cores with variable zoning are overgrown by oscillatory-zoned overgrowths from 5 to 60 μm wide.

The analysed zircons have moderate U and Th contents (Tab. 2). Most of the overgrowths have

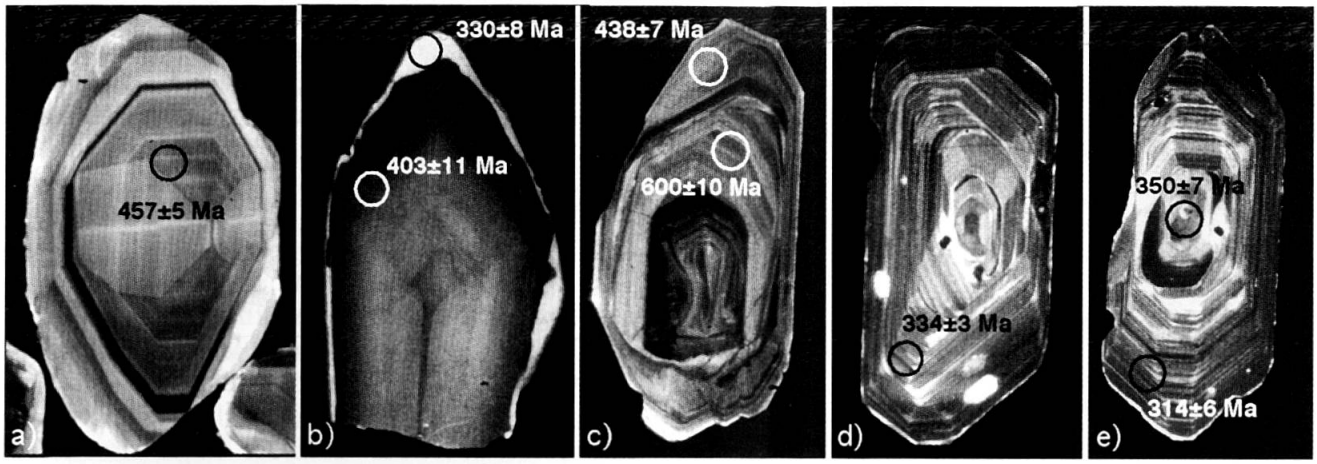

Fig. 4 Cathodoluminescence images of dated zircon crystals. Circles are 25 μm in diameter and indicate the pits of SHRIMP analyses. (a) Zircon from eclogite ARGI with magmatic zoning and undisturbed U–Pb age. (b) Zircon from eclogite ARGI in which the core preserves magmatic zoning but yield an age younger than the intrusion because of loss of lead during metamorphism. The bright rim either recrystallised or grew during metamorphism. (c) Zircon from metadacite ARGP with a composite inherited core surrounded by a magmatic overgrowth dating the crystallisation of the rock. (d) Zircon from metamonzonite ARGB, which preserves magmatic zoning and age. (e) Zircon from metamonzonite ARGB with a core that preserves an older Pb component. The magmatic overgrowth lost Pb most likely during Variscan metamorphism.

Th/U ratios between 0.1 and 0.3, while the cores have generally higher values. The zircon overgrowths yield ages around 440 Ma, whereas the cores contain older Pb components with ages scattering between 560 Ma and 2.2 Ga. The cores yielded concordant analyses at 560 Ma, 600 Ma and 700 Ma. The SHRIMP analyses of the oscillatory-zoned overgrowths cluster close to concordia with the exception of one data point (Fig. 5b). The concordant analyses define a mean $^{206}Pb/^{238}U$ age of 443 ± 3 Ma.

The magmatic origin of the rock is documented by the porphyritic texture and is supported by the euhedral shape and the oscillatory-zoning of the zircon crystals. The oscillatory-zoned overgrowths, which have rather homogeneous U and Th contents and have a magmatic Th/U ratio, are interpreted as new zircon growth on inherited cores at the time of magma crystallisation at 443 ± 3 Ma. The abundance of inherited cores of various ages indicates that the magma was saturated in Zr, as is generally observed in S-type magmas (e.g. WILLIAMS, 1998), and that the dacitic magma was likely produced by crustal re-melting. The oldest age measured (2.2 Ga) cannot be directly taken as evidence for Early Proterozoic crust in the area. In fact, zircon can survive repeated cycles of melting, deposition and metamorphism and a single, discordant zircon core does not have geological significance.

METAMONZONITE ARGB

Metamonzonite bodies or dykes crop out in the Gesso della Barra valley, in the central part of the GST (Fig. 2). These bodies were first reported by ROCCATI (1925) as "pyroxene-bearing porphyritic gneisses" and then mapped by Malaroda and coworkers as "biotite-amphibole embrechites" (CARRARO et al., 1970; MALARODA, 1970). An extensive outcrop of metamonzonite occurs at the Muraion Glacier (Fig. 2) and is surrounded by migmatites. Deformation is generally weak, but can locally be pervasive forming a banded rock with quartzo-feldspathic and mafic layers. Migmatisation is documented by a network of veinlets containing K-feldspar and amphibole, which are more abundant where the rock is strongly deformed.

The metamonzonites largely preserve magmatic texture (Fig. 3b) and mineralogy with centimetre-sized, euhedral K-feldspar and minor plagioclase with inclusions of magmatic biotite. The matrix contains relics of magmatic clinopyroxene partly replaced by late magmatic or metamorphic amphibole associated with biotite. Accessory minerals are apatite, zircon, allanite and opaques. According to the chemical analysis (Tab. 1) this sample has a trachyandesitic affinity and is characterised by high Mg and K contents, and enrichment in Th, Rb, Sr and Zr. Magmas of similar composition are known in several External Crystalline Massifs, including Pelvoux (BANZET, 1987;

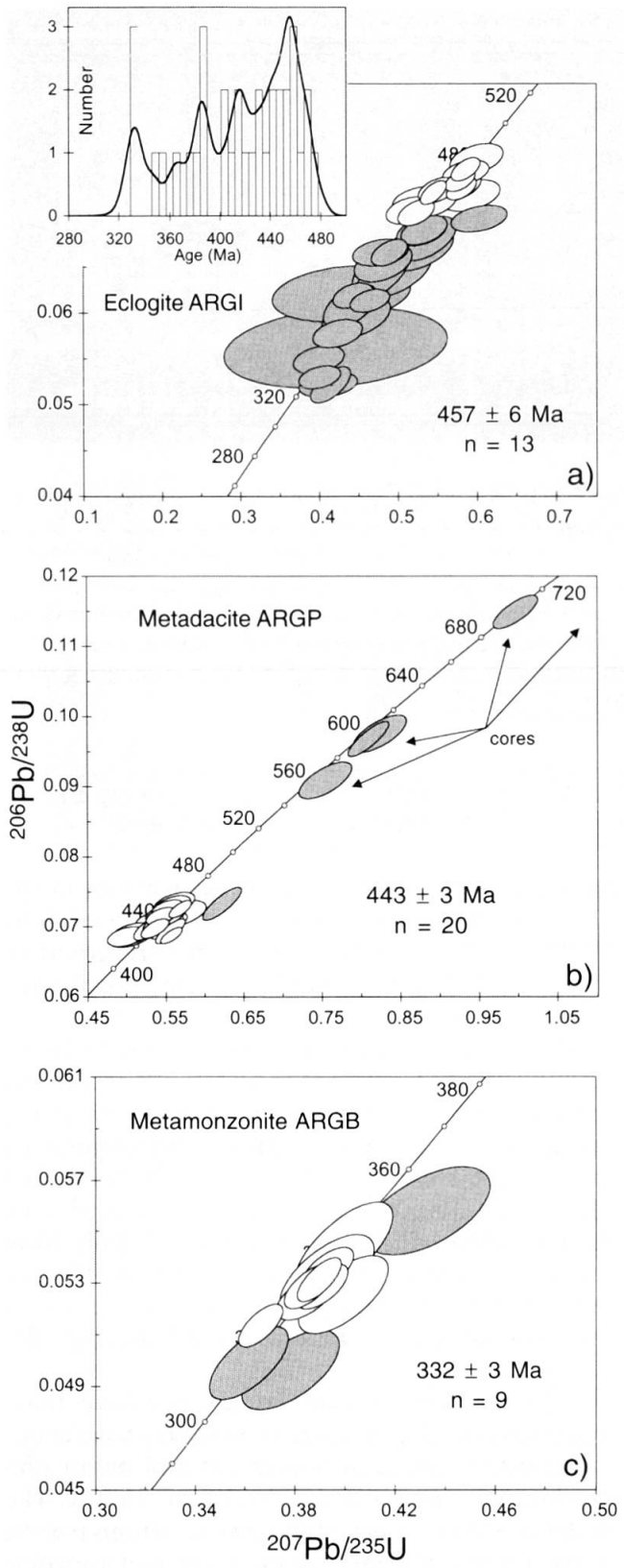

Fig. 5 Concordia plot for SHRIMP U–Pb data of (a) eclogite ARGI, (b) metadacite ARGP and (c) metamonzonite ARGB. The inset in (a) shows the histogram of the SHRIMP analyses with superimposed a cumulative probability curve. Data are plotted at 65% confidence level and mean ages are given at 95% confidence level. Data plotted in grey are excluded from the age calculation.

GUERROT and DEBON, 2000), Belledonne (DEBON et al., 1998), Aiguilles Rouges (BUSSY et al., 1998) and Aar (SCHALTEGGER, 1993). See DEBON and LEMMET (1999) for an extensive compilation and interpretation of the Mg-K magmatism in the Western Alps.

U–Pb data

The sample collected contains pink, large, euhedral zircons with a mean length-width ratio of 2.5. In CL, the zircons show a regular oscillatory zoning with bands parallel to the crystallographic faces (Figs 4d–e). Several crystals preserve inherited cores. SHRIMP analyses of 11 zircons revealed medium to high U (555–1261 ppm) and Th contents (272–609 ppm), and a rather uniform Th/U ratio (0.4–0.7: Tab. 2). One analysis corresponding to a zircon core (Fig. 4e) retains an older Pb component, whilst younger ages were obtained for two oscillatory-zoned zircon domains, which are suspected of having lost lead after magma crystallisation. The remaining nine analyses are normally distributed around 332 Ma and yield a concordant age of 332 ± 3 Ma (Fig. 5c).

The metamonzonite preserves magmatic mineral and textural relics. The zircons display regular oscillatory zoning, rather homogeneous U contents and Th/U ratios, both supporting a magmatic origin. Therefore, the age of 332 ± 3 Ma is interpreted as dating the crystallisation of the monzonite. Inheritance of older lead components is attributed to the preservation of zircon from the magma source in the Zr-saturated monzonitic magma. The young apparent ages measured in some zircon domains are best explained as lead loss due to either Variscan anatexis or to recent alteration.

Discussion

MAGMATIC EVOLUTION OF THE GESSO-STURA TERRAIN

The new geochronological results constrain the age of three major magmatic events in the Gesso-Stura Terrain (Fig. 7).

A. Intrusion of gabbros during Ordovician (459 ± 4 Ma). This age is the first dating of an eclogite protolith in the Argentera massif. A similar, even though imprecise, U–Pb age was previously obtained on zircon from a garnet-amphibolite of Madone de Fenestre (France), which gave a three-points discordia line with upper intercept at 471+40/–29 Ma and a geologically meaningless lower intercept (PAQUETTE et al., 1989). The Ordovician age was interpreted by the authors as

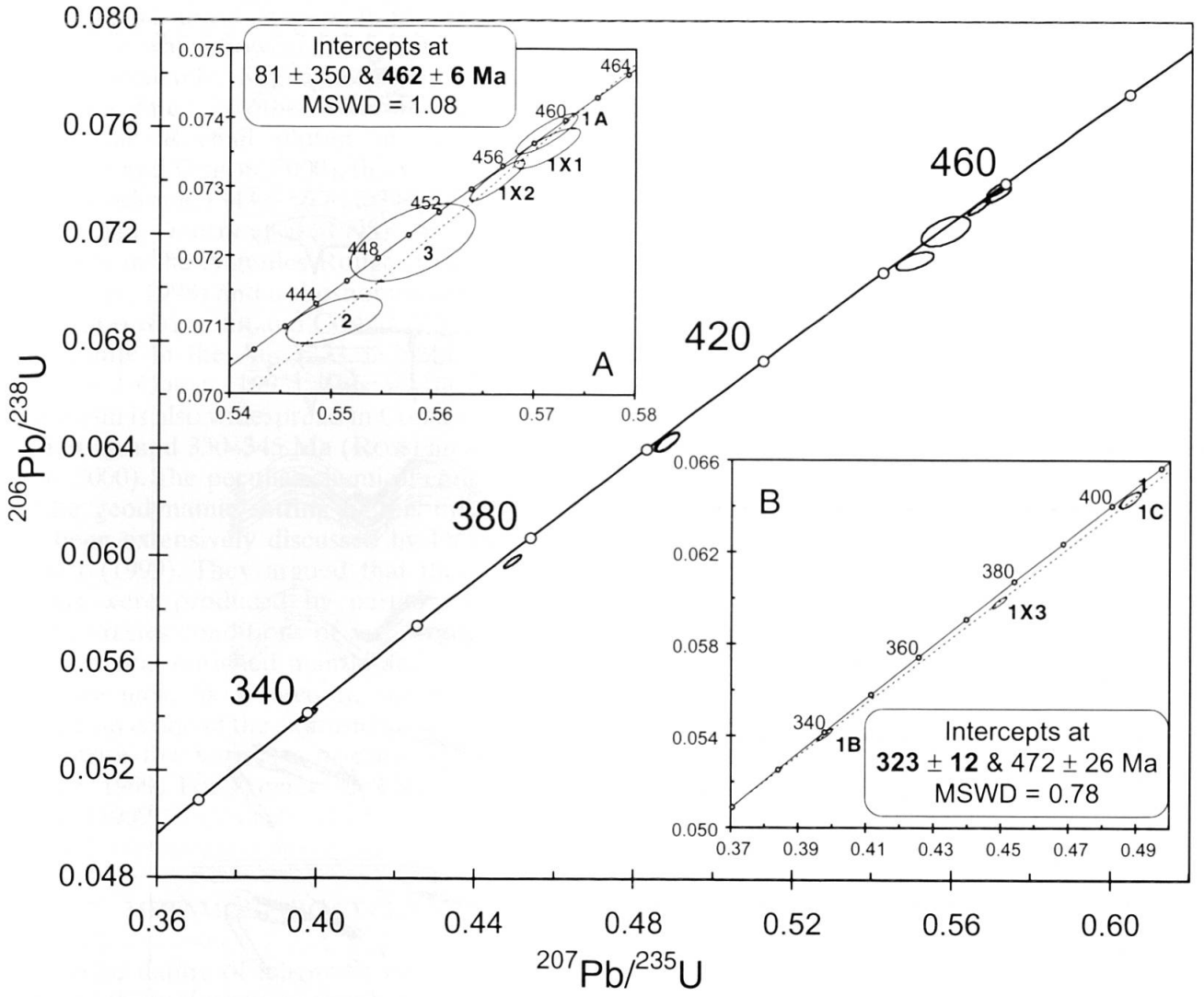

Fig. 6 Concordia plot for the ID-TIMS analyses of zircons from eclogite ARGI. Ellipses represent 2σ errors and mean ages are given at 95% confidence level. Analysis 2 represents a six-grain fraction, while the other analyses are from single grains. The age of magma crystallisation (462 ± 6 Ma) is obtained from the upper intercept defined by the five most concordant data points (inset A). The exclusion of analysis 1X1, which may be regarded as slightly biased by inherited lead, does not change the intercept age. The lower intercept is constrained by the four most discordant analyses (inset B) and is interpreted as maximum age for the Variscan metamorphism.

dating the intrusion of the magmatic precursor of the amphibolite. The same authors reported Ordovician mafic magmatism in the Belledonne and in the Aiguilles Rouges massif (473+28/–21 Ma and 453+3/–2 Ma, respectively) on the basis of discordia upper intercepts. An older ophiolitic sequence (496 ± 6 Ma; Chamrousse ophiolite) is reported in the Belledonne by MÉNOT et al. (1988). More recently, Ordovician metagabbros were dated by U–Pb in the Gotthard massif (467+5/–4 Ma; OBERLI et al., 1994), the Tavetsch unit (471+6/–7 Ma; OBERLI et al., 1994), the Aar massif (479 ± 5 Ma; ABRECHT et al., 1995) and in the Austroalpine Silvretta nappe (467 ± 14 Ma; POLLER, 1997). Because of the difference in age these Ordovician gabbros cannot be directly related to ophiolitic sequences such as Chamrousse (MÉNOT et al. 1988); the gabbros might have been isolated mafic bodies derived from subcontinental mantle. It is however likely that this mafic magmatism was produced by the opening of the Rheic ocean between Gondwana and Avalonia/Cadomia (VON RAUMER and STAMPFLI, 2000).

The igneous age obtained for the eclogite protolith indicates that the hosting orthogneiss ("anatexite") is older than the orthogneiss widespread in other external Crystalline Massifs (e.g. in the Aar-Gotthard), and whose igneous protolith is dated at around 450–440 Ma (e.g. BUSSY and VON RAUMER, 1993; SCHALTEGGER, 1993; SERGEEV et al., 1995). Therefore, the protolith of the orthogneiss in which the mafic magma intruded

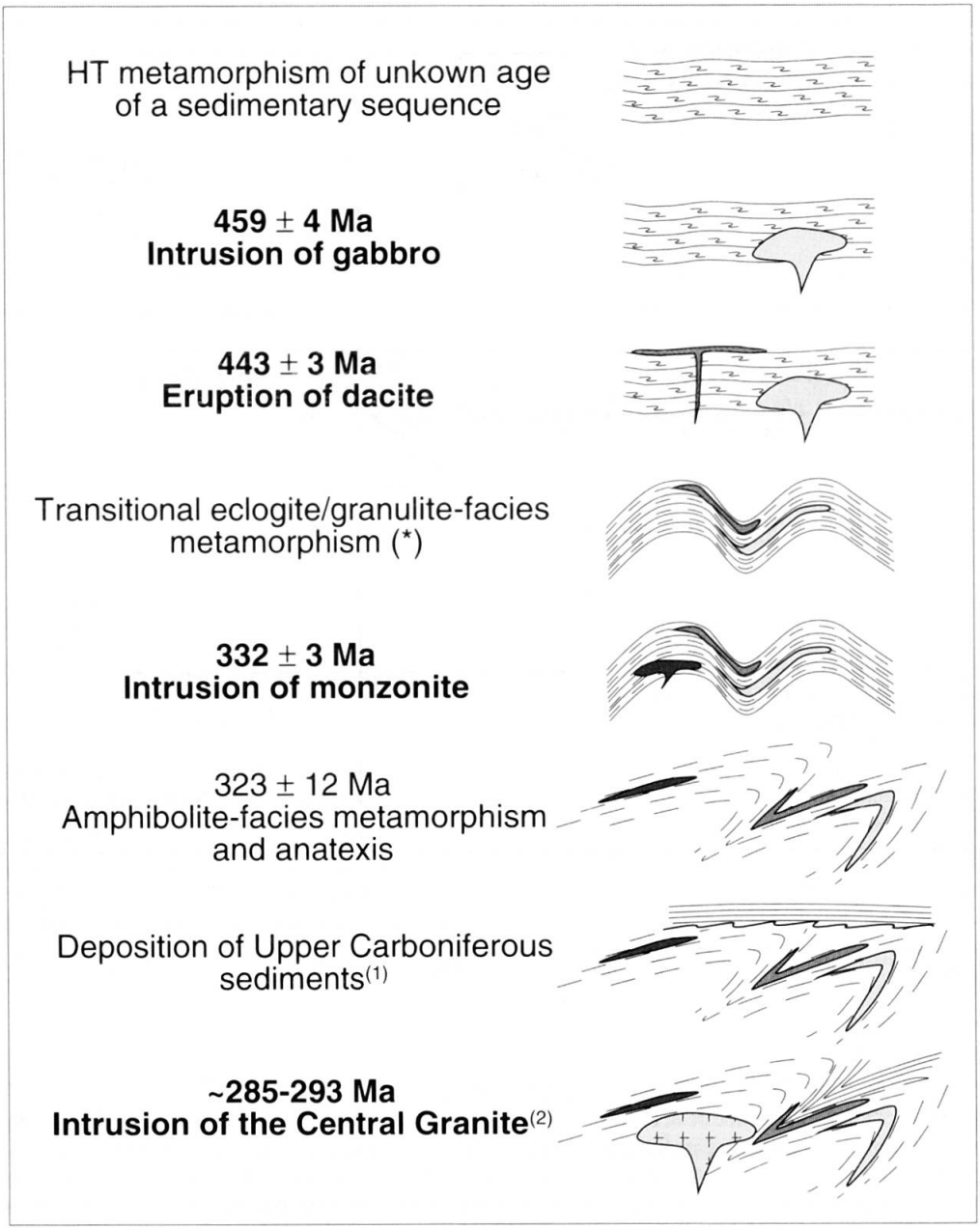

Fig. 7 Schematic evolution of the Gesso-Stura Terrain of the Argentera massif from Early Ordovician to Late Carboniferous. (*) The E-/G-facies metamorphism could have occurred before the intrusion of the dacite, in which case this Devonian event was a HT event only. Data from (1) FAURE-MURET (1955) and (2) FERRARA and MALARODA (1969). See text for discussion.

should be at least lower Ordovician in age and possibly even older.

B. Dacitic volcanism in the Late Ordovician (443 ± 3 Ma). The crystallisation age of the metadacite is the first report of Ordovician volcanism in the Argentera massif. However, acid volcanics of this age have been reported elsewhere in the Pennine area and the Eastern Alps (see VON RAUMER, 1998, for a review). This volcanism may be, at least in part, related to the arc Ordovician granitoids (VON RAUMER, 1998), which have been extensively documented in the pre-Variscan basement of the External Crystalline Massifs (Aiguilles Rouges: BUSSY and VON RAUMER, 1993; Aar: SCHALTEGGER, 1993; Gotthard: SERGEEV et al., 1995). This Late Ordovician acid magmatism appears to be the final episode of a magmatic cycle that lasted over the whole Ordovician. Several geotectonic settings have been proposed for this magmatism (VON RAUMER and NEUBAUER, 1993). In a recent compilation, VON RAUMER (1998) suggested that they might represent the late product of an active Cambro–Ordovician Gondwana margin.

C. Intrusion of monzonitic magmas in the Carboniferous (332 ± 3 Ma). This acid magmatism might be related to the basic magmatism in the

Bousset-Valmasque Complex, in the SE part of the GST, for which however no geochronological data are available. Similar Mg-rich syenitoids have been dated in other External Crystalline Massifs: the Rochail pluton in the Pelvoux (GUERROT and DEBON, 2000), the Visean plutons in the Belledonne (343 ± 16 Ma, 341 ± 13 Ma and 335 ± 13 Ma; DEBON et al., 1998), the Pormenaz monzonite in the Aiguilles Rouges (332 ± 2 Ma; BUSSY et al., 1998) and a shoshonitic suite (334 ± 2.5 Ma; SCHALTEGGER and CORFU, 1992) and the Tödi granite in the Aar (333 ± 2 Ma; SCHALTEGGER and CORFU, 1995). This Variscan K-rich magmatism is also widespread in Corsica where is dated at around 330–345 Ma (ROSSI and CARMIGNANI, 2000). The peculiar chemical composition and the geodynamic setting of this magmatism have been extensively discussed by DEBON and LEMMET (1999). They argued that these K-rich magmas were produced by partial melting at granulite-facies conditions of a source including subcontinental enriched mantle and continental crust. The most likely tectonic setting for such magmatism is one of the extensional episodes that characterise the Variscan orogeny (DEBON and LEMMET, 1999). For a review see also VON RAUMER et al. (1999).

METAMORPHIC CYCLES

The precise dating of magmatic events brackets the age of the various metamorphic cycles that affected the Argentera massif (Fig. 7).

1. Granulite-facies metamorphism. The xenoliths in the metadacite document a HT event that predates the Ordovician emplacement of the dacite at 443 ± 3 Ma. This HT event could either have produced the dacitic magma or be older and maybe correlated to the anatexis dated at 456 ± 2 Ma in the Aar massif (SCHALTEGGER, 1993). Migmatites of possible pre-Ordovician age exist in the NW of the Argentera massif.

2. E/G-facies metamorphism. The dacite contains a garnet-bearing assemblage recording a HP granulitic event that, in the more deformed facies, has been interpreted as pre-Variscan (BIERBRAUER, 1995). It seems likely that this event corresponds to the E/G-facies metamorphism recorded in the Meris eclogite and in the rocks of Lago Frisson (LOMBARDO et al., 1997). This hypothesis would imply that the E/G-facies metamorphism occurred after the eruption of the dacite (443 ± 3 Ma) and before the intrusion of the metamonzonite (332 ± 3 Ma), which does not record the E/G-facies event. According to this interpretation, the GST recorded a similar evolution to that of the French Massif Central, where a single HP-HT event of Devonian age has been described (e.g. PAQUETTE et al., 1995). On the contrary, if the garnet-bearing assemblage in the dacite is interpreted as post-eclogitic, then the E/G-facies metamorphism recorded in the Meris eclogite occurred before the emplacement of the dacite, between ~459 and ~443 Ma. In such a case, two HP-HT events were recorded in the GST: an eclogite-facies event of Ordovician age, and a non-eclogitic event of Devonian age. In this second scenario the evolution of the GST is similar to that described in the Aar-Gotthard Massif and the first of these events could be correlated with the hypothetical eclogite-facies event dated in the Gotthard by U–Pb and Sm–Nd at around 460–470 Ma (GEBAUER, 1993).

A previous attempt to date the eclogite-facies metamorphism in the Argentera massif provided an age of 424 ± 4 Ma (PAQUETTE et al., 1989). However, this age results from a lower intercept of a discordia line obtained by U–Pb analysis of zircon from a hornblende-plagioclase amphibolite that had no relics of HP minerals. Moreover, the same authors obtained an age of 351 ± 1 Ma from "metamorphic looking" zircons of a retrogressed eclogite which was also interpreted as a possible date of the HP metamorphic event. It is likely that these age determinations using multigrain fractions lead to meaningless ages because of complex mixing relationships of at least three age components.

3. Variscan amphibolite-facies metamorphism and anatexis. A maximum age of 323 ± 12 Ma for the Variscan amphibolite-facies metamorphism, which culminated with widespread anatexis, is inferred from the lower intercept obtained by ID-TIMS analysis of zircon from the Meris eclogite. This age is supported by the ~330 Ma zircon rims from the same rocks, which were analysed with SHRIMP. The intrusion at 332 ± 3 Ma of the monzonite, a rock that underwent anatexis, also points to an amphibolite-facies Variscan metamorphism of mid to Late Carboniferous age.

Our results for the GST differ from the ~350 Ma age previously suggested for the Variscan metamorphic peak on the basis of poorly constrained Ar–Ar dating of muscovite from gneisses of the Tinée Complex (MONIÉ and MALUSKI, 1983). This discrepancy could be explained by a difference in time of metamorphism in the two complexes, which are in fact separated by a major tectonic line. The deposition of Upper Carboniferous (Middle Stephanian) sediments in the French part of the GST (FAURE-MURET, 1955, p. 153) constrains the age of the Variscan metamorphism to the Mid–Late Carboniferous (Na-

murian or Westphalian). The intrusion of the cross cutting Central Granite at around 285–293 Ma (Rb–Sr whole rock and mineral isochron; FERRARA and MALARODA, 1969) is a further young age limit for the Variscan amphibolite-facies metamorphism. In the Mont Blanc massif, Variscan metamorphism and anatexis have been precisely dated with monazite U–Pb at 317 ± 2 Ma (BUSSY and VON RAUMER, 1993).

In summary, this geochronological study allows constraining the geological history of the GST during the Paleozoic, which evolved through at least three magmatic events and two or three metamorphic events.

IMPLICATIONS FOR ZIRCON GEOCHRONOLOGY

Some of the CL and isotopic data presented are relevant for the further study of U–Th–Pb systematics in zircon. The zircons from the metadacite show no evidence of lead loss after crystallisation, even though the host rock underwent pervasive Variscan anatexis and possibly static E/G-facies metamorphism (> 800 °C). The zircons preserve original magmatic oscillatory zoning and isotopic composition. On the other hand, the zircons from the metamonzonite have oscillatory-zoned domains that lost lead possibly during the Variscan amphibolite-facies event. Similarly, the zircons recovered from the eclogite preserve magmatic CL zoning even in domains that lost lead during one or more metamorphic events after crystallisation.

The absence of lead loss in the magmatic zircon from the metadacite confirms that the U–Th–Pb system in zircon may remain closed even though the host rock is heated to relatively high temperatures. This is in agreement with experimental data demonstrating that Pb diffusion in zircon occurs only at temperatures > 900 °C (CHERNIAK and WATSON, 2001; LEE et al., 1997). Perturbation of the U–Pb system at lower temperatures, as in the case of the zircon from the eclogite or the metamonzonite, is most likely due to processes such as fracturing and fluid percolation.

CL imaging of zircons reveals their internal zoning and has often been used to identify multi-growth histories, recrystallisation, annealing, resorption or lead loss in zircon crystals (e.g. (HOSKIN and BLACK, 2000; RUBATTO and GEBAUER, 2000; SCHALTEGGER et al., 1999; VAVRA et al., 1996; VAVRA et al., 1999). The zircons of the Meris eclogite and, at least in part, those of the metamonzonite are a clear example in which magmatic zoning remained pristine even though widespread lead loss occurred, not only in the rims, but even in crystal centres. These zircons do not show any microfractures or zoned affected by leaching or annealing as described by VAVRA et al. (1999) and SCHALTEGGER et al. (1999), neither are they particularly Th or U rich to suggest Pb loss because of radiation damage. This unusual case demands a certain caution in interpreting CL zoning when precise in-situ isotope analysis are not available.

Summary

The GST of the Argentera massif has a metamorphic basement of Early Ordovician or older age, which, similarly to other External Crystalline Massifs, was intruded by gabbroic magmas at 459 ± 4 Ma. This basement was then involved in an orogenic cycle that produced eclogite-facies assemblages in the gabbros and garnet-kyanite granulites from the sedimentary and magmatic rocks (T > 800 °C, P ~1.6–1.8 GPa). This metamorphism occurred either shortly after the gabbro intrusion or after the eruption of dacites at 443 ± 3 Ma. These volcanic rocks, which sampled granulite-facies xenoliths from the mid-lower crust beneath the Argentera massif, appear to be coeval with the arc Ordovician magmatism widely documented in the pre-Variscan basement of the External Crystalline Massifs. Monzonitic intrusions were emplaced at 332 ± 3 Ma as part of a large-scale Variscan extension that is recorded in most of the External Crystalline Massifs and in Corsica. This early history of the Argentera massif has been largely obliterated by post 323 ± 12 Ma pervasive Variscan amphibolite-facies metamorphism accompanied by widespread anatexis. Deposition of Upper Carboniferous sediments and the intrusion of the Central Granite at the Carboniferous-Permian boundary marked the end of the Variscan orogeny.

Our approach has shown that zircon that underwent one or more thermal perturbations at temperature of 700–850 °C may lose a significant amount of lead. This lead loss can affect even domains that show no evidence of fracturing, leaching, annealing or recrystallisation. U–Pb system perturbation can occur either during metamorphism or in recent times and is best identified by combining conventional ID-TIMS and SHRIMP ion microprobe analysis.

Acknowledgements

Whole rock chemical analyses of the samples dated were performed at the Dipartimento di Georisorse e

Territorio, Università di Udine. Mark Fanning is thanked for supervision of part of the SHRIMP work, W. Wittwer for assisting with the mineral separation and A. von Quadt for mass spectrometer maintenance. G. Ghiglione kindly shared information on the metadacites. B. Lombardo acknowledges the support of the Centro di Studi sulla Geodinamica delle Catene Collisionali of the Consiglio Nazionale delle Ricerche. The constructive reviews of J. von Raumer and an anonymous reviewer improved the manuscript.

References

ABRECHT, J., BIINO, G.G. and SCHALTEGGER, U. (1995): Building the European continent: Late Proterozoic–Early Paleozoic accretion of the Central Alps of Switzerland. Terra Abstracts 7, 105.

BANZET, G. (1987): Interactions croûte-manteau et genèse du plutonisme subalcalin du Haut-Dauphiné occidental (massifs cristallins externes, Alpes): vaugnérites, durbachites et granitoïdes magnésio-potassiques. Géologie Alpine 63, 95–117.

BIERBRAUER, K. (1995): Quantitative Verteilung von Deformation und Strukturen in migmatitischen Gesteinen der Mittel/Unterkruste. 3D-Strukturmodellierung im kristallinen Argentera Massiv in der Externzone der Westalpen. Unpubl. Doctoral thesis, University of Würzburg, 225 pp.

BOGDANOFF, S. (1986): Evolution de la partie occidentale du massif cristallin externe de l'Argentera. Place dans l'arc alpin. Géol. France 4, 433–453.

BUSSY, F., DÉLITROZ, D., FELLAY, R. and HERNANDEZ, J. (1998): The Pormenaz monzonite (Aiguilles-Rouges, Western Alps): an additional evidence for a 330 Ma-old magnesio-potassic magmatic suite in the Variscan Alps. Schweiz. Mineral. Petrogr. Mitt. 78, 193–194.

BUSSY, F. and VON RAUMER, J.F. (1993): U–Pb dating of Palaeozoic events in the Mont-Blanc crystalline massif, Western Alps. Terra Nova 5, 382–383.

CARRARO, F., DAL PIAZ, G.V., FRANCESCHETTI, B., MALARODA, R., STURANI, C. and ZANELLA, E. (1970): Note Illustrative della Carta Geologica del Massiccio dell'Argentera alla scala 1:50000. Mem. Soc. Geol. It. 9, 557–663.

CHAPPELL, B.W. and WHITE, A.J.R. (1992): I- and S-type granites in the Lachlan Fold Belt. Trans. Royal Soc. Edinburgh, Earth Sci. 83, 1–26.

CHERNIAK, D.J. and WATSON, E.B. (2001): Pb diffusion in zircon. Chem. Geol. 172, 5–24.

COLOMBO, F., GHIGLIONE, G. and COMPAGNONI, R. (1993): Relitti di porfidi granitici a xenoliti granulitici nelle migmatiti dell'Argentera (Alpi Marittime). Plinius, Suppl. to Eur. J. Mineral. 10, 113–116.

COMPSTON, W., WILLIAMS, I.S., KIRSCHVINK, J.L., ZHANG, Z. and MA, G. (1992): Zircon U–Pb ages for the Early Cambrian time-scale. J. Geol. Soc. London 149, 171–184.

DEBON, F., GUERROT, C., MÉNOT, R.-P., VIVIER, G. and COCHERIE, A. (1998): Late Variscan granites of the Belledonne massif (French Western Alps): an Early Visean magnesian plutonism. Schweiz. Mineral. Petrogr. Mitt. 78, 67–85.

DEBON, F. and LEMMET, M. (1999): Evolution of Mg/Fe ratios in the Late Variscan plutonic rocks from the External Crystalline Massifs of the Alps (France, Italy, Switzerland). J. Petrol. 40, 1151–1185.

FAURE-MURET, A. (1955): Etudes géologiques sur le massif de l'Argentera-Mercantour et ses enveloppes sedimentaires. Mémoires de la Carte géologique de France, 336 pp.

FERRARA, G. and MALARODA, R. (1969): Radiometric age of granitic rocks from the Argentera Massif (Maritime Alps). Boll. Soc. Geol. It. 88, 311–320.

GEBAUER, D. (1993): The pre-Alpine evolution of the continental crust of the Central Alps – An overview. In: VON RAUMER, J.F. and NEUBAUER, F. (eds): Pre-Mesozoic geology in the Alps. Springer. Berlin Heidelberg, 93–117.

GHIGLIONE, G. (1990): Studio geologico dell'alta Valle della Rovina. Unpubl. Master Thesis, Turin University, 393 pp.

GUERROT, C. and DEBON, F. (2000): U–Pb zircon dating of two contrasting Late Variscan plutonic suites from the Pelvoux massif (French Western Alps). Schweiz. Mineral. Petrogr. Mitt. 80, 249–256.

HOLLAND, T.J.B. (1980): The reaction albite = jadeite + quartz determined experimentally in the range 600–1200 °C. Am. Mineral. 64, 129–134.

HOSKIN, P.W.O. and BLACK, L.P. (2000): Metamorphic zircon formation by solid-state recrystallization of protolith igneous zircon. J. Metamorphic Geol. 18, 423–439.

LEE, J.K.W., WILLIAMS, I.S. and ELLIS, D.J. (1997): Pb, U and Th diffusion in natural zircon. Nature 390, 159–161.

LOMBARDO, B., COLOMBO, F., COMPAGNONI, R., GHIGLIONE, G. and RUBATTO, D. (1997): Relics of pre-Variscan events in the Malinvern-Argentera Complex, Argentera Massif, Western Alps. Quaderni di Geodinamica Alpina e Quaternaria 4, 66.

LUDWIG, K.R. (2000): Isoplot/Ex version 2.4. A geochronological toolkit for Microsoft Excel, Berkeley Geochronological Centre Spec. Pub., 1–56.

MALARODA, R. (1970): Carta geologica del massiccio dell'Argentera. Firenze, Litografia Artistica Cartografica.

MALARODA, R. (1991): Gli gneiss pseudoporfido, particolare tipo litologico dell'Argentera meridionale. Gli affioramenti del bacino di Beonia (Bieugne) (Alpes-Maritimes, Francia). Atti della Accademia dei Lincei, Classe di Scienze Fisiche, Matematiche e Naturali s. 9, 1, 129–152.

MALARODA, R. (1992): Les gneiss-pseudoporphyres du bassin de la Vésubie (Alpes-Maritimes, France). Atti della Accademia dei Lincei, Classe di Scienze Fisiche, Matematiche e Naturali s. 9, 1, 221–244.

MALARODA, R. (1996): The pseudoporphyric gneisses of the Gordolasque and upper Merveilles valleys (Alpes-Maritimes, France). Atti della Accademia dei Lincei, Rendiconti di Scienze Fisiche, Matematiche e Naturali s. 9, 7, 101–158.

MALARODA, R. (1999): L'Argentera meridionale – Memoria illustrativa della "Geological Map of the Southern Argentera Massif (Maritime Alps) 1:25000". Mem. Sci. Geol. 51, 231–241.

MÉNOT, R.P., PEUCAT, J.J., SCARENZI, D. and PIBOULE, M. (1988): 496 Ma age of plagiogranites in the Chamrousse ophiolite complex (external crystalline massifs in the French Alps): evidence of a Lower Palaeozoic oceanization. Earth Planet. Sci. Lett. 88, 82–92.

MONIÉ, P. and MALUSKI, H. (1983): Données géochronologiques ^{39}Ar–^{40}Ar sur le socle anté-permien du massif de l'Argentera-Mercantour (Alpes-Maritimes, France). Bull. Soc. géol. France 7, 25, 247–257.

OBERLI, F., MEIER, M. and BIINO, G.G. (1994): Time constraints on the pre-Variscan magmatic/metamorphic evolution of the Gotthard and Tavetsch units derived from U–Pb results. Schweiz. Mineral. Petrogr. Mitt. 74, 483–488.

PAQUETTE, J.-L., MÉNOT, R.-P. and PEUCAT, J.-J. (1989): REE, Sm–Nd and U–Pb zircon study of eclogites from the Alpine External Massifs (Western Alps): evidence for crustal contamination. Earth Planet. Sci. Lett. 96, 181–198.

PAQUETTE, J.-J., MONCHOUX, P. and COUTURIER, M. (1995): Geochemical and isotopic study of a norite-eclogite transition in the European Variscan belt: Implications for U–Pb zircon systematics in metabasic rocks. Geochim. Cosmochim. Acta 59, 1611–1622.

POLLER, U. (1997): U–Pb single zircon study of gabbroic and granitic rocks of the Val Barlas-ch (Silvretta nappe, Switzerland). Schweiz. Mineral. Petrogr. Mitt. 77, 351–359.

POWELL, R. (1985): Regression diagnostics and robust regression in geothermometer/geobarometer calibration: the garnet-clinopyroxene geothermometer revisited. J. Metamorphic Geol. 3, 231–243.

ROCCATI, A. (1925): Il Massiccio Cristallino delle Alpi Marittime. Bollettino del Club Alpino Italiano 42, 189–241.

ROMAIN, J. (1982): Le Massif du Mercantour. Guide géologique. Serre, Nice. 106 pp.

ROSSI, P. and CARMIGNANI, L. (2000): Carta Geologico Strutturale della Sardegna e della Corsica. 1:500'000, Litografia Artistica Cartografica, Firenze.

RUBATTO, D. and GEBAUER, D. (2000): Use of Cathodoluminescence for U–Pb zircon dating by ion microprobe: some examples from the Western Alps. In: PAGEL, M., BARBIN, V., BLANC, P. and OHNENSTETTER, D. (eds): Cathodoluminescence in Geosciences. Springer. Berlin Heidelberg New York, 373–400.

RUBATTO, D., GEBAUER, D. and FANNING, M. (1998): Jurassic formation and Eocene subduction of the Zermatt-Saas-Fee ophiolites: Implications for the geodynamic evolution of the Central and Western Alps. Contrib. Mineral. Petrol. 132, 269–287.

SCHALTEGGER, U. (1993): The evolution of the polymetamorphic basement in the Central Alps unravelled by precise U–Pb zircon dating. Contrib. Mineral. Petrol. 113, 466–478.

SCHALTEGGER, U. and CORFU, F. (1992): The age and the source of the late Hercynian magmatism in the central Alps: evidence from precise U–Pb age and initial Hf isotopes. Contrib. Mineral. Petrol. 111, 329–344.

SCHALTEGGER, U. and CORFU, F. (1995): Late Variscan "Basin and Range" magmatism and tectonics in the Central Alps: evidence from U–Pb geochronology. Geodin. Acta 8, 82–98.

SCHALTEGGER, U., FANNING, M., GÜNTHER, D., MAURIN, J.C., SCHULMANN, K. and GEBAUER, D. (1999): Growth, annealing and recrystallization of zircon and preservation of monazite in high-grade metamorphism: conventional and in-situ U–Pb isotope, cathodoluminescence and microchemical evidence. Contrib. Mineral. Petrol. 134, 186–201.

SERGEEV, S.A., MEIER, M. and STEIGER, R.H. (1995): Improving the resolution of single grain U/Pb dating by use of zircon extracted from feldspar: application to the Variscan magmatic cycle in the Central Alps. Earth Planet. Sci. Lett. 134, 37–51.

VAVRA, G., GEBAUER, D., SCHMIDT, R. and COMPSTON, W. (1996): Multiple zircon growth and recrystallization during polyphase Late Carboniferous to Triassic metamorphism in granulites of the Ivrea Zone (Southern Alps): an ion microprobe (SHRIMP) study. Contrib. Mineral. Petrol. 122, 337–358.

VAVRA, G., SCHMIDT, R. and GEBAUER, D. (1999): Internal morphology, habit and U–Th–Pb microanalysis of amphibolite to granulite facies zircons: geochronology of the Ivrea Zone (Southern Alps). Contrib. Mineral. Petrol. 134, 380–404.

VON RAUMER, J.F. (1998): The Paleozoic evolution in the Alps: from Gondwana to Pangea. Geol. Rundsch. 87, 407–435.

VON RAUMER, J.F., ABRECHT, J., BUSSY, F., LOMBARDO, B., MÉNOT, R.-P. and SCHALTEGGER, U. (1999): The Paleozoic metamorphic evolution of the Alpine External Massifs. Schweiz. Mineral. Petrogr. Mitt. 79, 5–22.

VON RAUMER, J.F. and NEUBAUER, F. (1993): Late Precambrian and Pelaeozoic evolution of the Alpine basement – An overview. In: VON RAUMER, J.F. and NEUBAUER, F. (eds): Pre-Mesozoic geology in the Alps. Springer. Berlin Heidelberg, 625–639.

VON RAUMER, J.F. and STAMPFLI, G.M. (2000): Comparing the peri-Gondwanan evolution of pre-Variscan domains. Basement Tectonics 15, A Coruña, Spain, Program and Abstracts, 18–20.

WILLIAMS, I. (1998): U–Th–Pb geochronology by ion microprobe. In: MCKIBBEN, M.A., SHANKS III, W.C. and RIDLEY, W.I. (eds): Application of microanalytical techniques to understanding mineralizing processes. Reviews in Economic Geology 7, 1–35.

Manuscript received December 4, 2000; revision accepted June 6, 2001.
Editorial handling: Jan D. Kramers